Optical frequency transfer over submarine fiber links

Research Article Vol. 5, No. 8 / August 2018 / Optica 893

Optical frequency transfer over submarine fiber links

Cecilia Clivati,[1] Anna Tampellini,[1,2] Alberto Mura,[1] Filippo Levi,[1] Giuseppe Marra,[3] Pauline Galea,[4] André Xuereb,[5] and Davide Calonico[1,*]

[1]Istituto Nazionale di Ricerca Metrologica, Strada delle Cacce 91, 10135 Turin, Italy
[2]Politecnico di Torino, Corso Duca degli Abruzzi 24, 10129 Turin, Italy
[3]National Physical Laboratory, Hampton Road, Teddington TW11 0LW, UK
[4]Department of Geosciences, University of Malta, Msida MSD 2080, Malta
[5]Department of Physics, University of Malta, Msida MSD 2080, Malta
*Corresponding author: d.calonico@inrim.it

Received 23 February 2018; revised 11 May 2018; accepted 11 May 2018 (Doc. ID 324578); published 25 July 2018

Bidirectional phase-stabilized optical fiber links allow state-of-the-art optical clocks to be compared on a continental scale. However, intercontinental comparisons are still based on satellite techniques, preventing optical clocks from being compared without degradation. We performed the first optical frequency transfer experiment over submarine links, measuring levels of environmentally induced noise substantially lower than for on-land links. From these measurements, we predict the transfer stability that can be achieved over transoceanic links. We also performed the first optical frequency transfer over fibers installed in power cables, observing optical perturbations caused by the high-voltage field. Finally, we show that the low background noise of fibers on the seafloor allows applications in geophysical sensing.

OCIS codes: (120.3940) Metrology; (060.2360) Fiber optics links and subsystems; (060.2330) Fiber optics communications.

https://doi.org/10.1364/OPTICA.5.000893

1. INTRODUCTION

Fiber-based frequency transfer techniques have enabled the comparison of state-of-the-art optical atomic clocks over thousands of kilometers (km) without degradation. Satellite-based techniques, traditionally used for long distance comparison of frequency standards, are no longer capable of supporting the required accuracy of optical clocks, currently at the 10^{-18} level [1,2]. Optical fiber links will thus play an instrumental role in the redefinition the second based on optical transitions [3] and the development of global timescales based on optical clocks.

Recently, the first fiber-based remote atomic clock comparisons were performed [4–8]. In Europe, a network of research facilities connected on a global scale via optical fiber is under development [6–10]. Fiber-based frequency dissemination techniques have also been adopted in other science areas, such as radioastronomy [11–13] and spectroscopy [14–17]. However, one of the greatest outstanding challenges toward a global frequency distribution network is bridging transoceanic distances using frequency-transfer over submarine fiber cables.

Until this work, fiber-based optical frequency transfer experiments were performed only on telecommunication links installed on land. Fiber cables on land are typically installed in ducts for utility distribution, such as gas and electricity, often running across metropolitan areas and along highways. Optical fibers are sensitive to temperature variations [18], vibrations, and acoustic noise [19]. All these perturbations cause the phase of the transmitted optical signal to change. Several approaches have been adopted to suppress this environmentally-induced optical phase noise, which prevents clocks from being compared. In the most commonly used solution, the signal is transferred to the remote end and partially reflected back in the same fiber. The optical phase noise accumulated during a round trip of the light is measured by comparing at the transmitter end the returned optical signal with that injected in the fiber. The frequency of the light injected in the fiber is then actively adjusted with an actuator such that the resulting round-trip noise is suppressed. If the noise is identical between the two directions of propagation, compensating for the round-trip noise ensures that the noise at the far end of the fiber is also suppressed [20]. In long fiber links, bidirectional amplifiers are used to compensate for the loss introduced by the fiber (0.2 dB/km). An alternative approach consists of performing a two-way comparison, where two laser signals are sent in opposite directions through the fiber. For perturbations much slower than the speed of propagation of light in the fiber, the induced phase changes measured at each end are identical. By comparing these signals, the noise of the fiber is rejected, while frequency changes of the lasers are still detected [21].

In both techniques, the highest compensation is achieved when the noise is the same in the forward and backward propagation. This condition is met in fully bidirectional links, where the light is propagated in both directions through the same fiber.

This is different from the standard telecommunication link topology where separated fibers are used for each direction of propagation and unidirectional optical amplifiers are installed along the link. Optical links designed for metrological applications and installed on land require replacing unidirectional with bidirectional amplifiers. However, this is not feasible for submarine links resting on the ocean floor. Thus, a fully bidirectional link cannot be implemented, and two separate fibers have to be used instead. However, partial compensation of the fiber noise can be achieved if sufficient correlation exists between the two directions of propagation [22].

Here, we show the first optical frequency transfer experiment over two submarine telecommunication links in the Mediterranean Sea, of lengths 96.4 km and 117.5 km. One of these links is installed inside a high-voltage (HV) cable, and we observed large optical phase changes induced by the strong electric field. Time and frequency transfer experiments were previously performed over submarine fibers using passive listening of the data stream in synchronous telecom networks [23,24]. Our measurements report on the first characterization of submarine fibers both with high-resolution spectral and time-domain analysis.

The noise we measured over the submarine links enables us to perform quantitative predictions on the level of transfer stability that can be achieved over transcontinental distances when two separate fibers are used for the two directions of propagation. We calculate that intercontinental comparisons of atomic clocks can be performed with the same or lower instability than satellite techniques, but in a ∼100 times shorter measurement time.

2. OPTICAL PHASE NOISE IN SUBMARINE FIBER CABLES

We characterized the environmentally induced phase noise of two submarine cables following two different routes between Malta and Sicily (Italy). The first link (L1) is 96.4 km long, running under the seafloor for most of its length, with less than 2 km on land. The second (L2) consists of two sections, a 98.5-km-long link installed under the seafloor and a 19-km-long section on land. The submarine section of L2 is installed inside a three-core copper cable used for HV electricity distribution [25]. Both L1 and L2 use standard telecommunication fiber and are buried under the seafloor at a depth of 1 m. In shallow waters, cables are typically buried to reduce the risk of damage by boat anchors and trawling by fishing vessels. In deeper waters, cables are installed on or below the seafloor, depending on the seafloor surface. The measurement setup was placed in Malta, with the fibers joined at the far end in Sicily, such that 192.8-km-long and 235-km-long loops were formed. A map of the two testbeds is shown in Fig. 1.

We injected light from an ultra-stable laser into the fiber from the Malta end and measured the noise of the submarine fiber by phase comparing the light returned after a round trip with that of the laser. The coherence length of the laser is substantially longer than the length of the link such that the phase changes of the laser, over the round-trip time, are negligible.

A detailed sketch of the full experimental apparatus is shown in Fig. 2. We generated the ultra-stable light at the University of Malta by locking a fiber laser at 1542.14 nm (laser 1) to a high-finesse transportable Fabry–Perot cavity [26] using the Pound–Drever–Hall technique. Further details are given in Supplement 1. We implemented a noise-compensation loop to

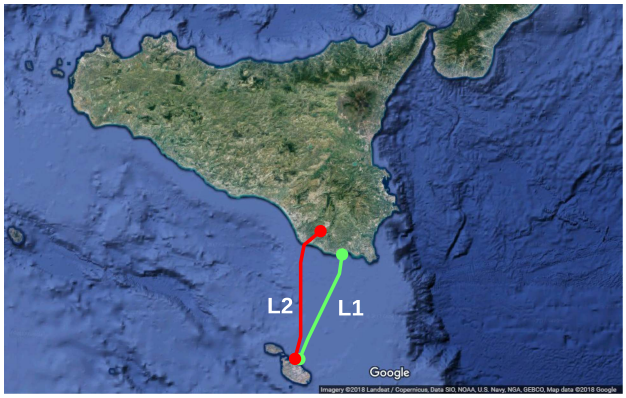

Fig. 1. Map of the two testbeds: L1 (green) is a 96.4-km-long telecom cable deployed almost entirely in sea. L2 (red) is a telecom cable housed in a HV line. The length is 117.5 km, of which 19 km are on land. The seafloor is extremely flat in the area, with a maximum depth of 200 m. (Imagery © 2018 Landsat/Copernicus, Data SIO, NOAA, U.S. Navy, NGA, GEBCO, IBCAO, Map data © 2018 Google.)

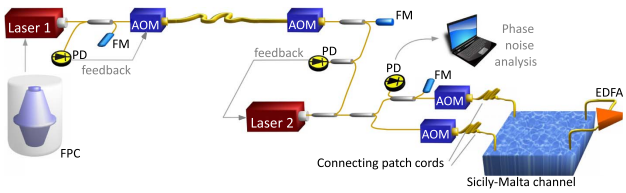

Fig. 2. Sketch of our experiment: ultrastable radiation was generated by locking a fiber laser (laser 1) to a Fabry–Perot cavity (FPC), then sent from University of Malta to the landing station in Malta via a Doppler-stabilized link and here regenerated by a second fiber laser (laser 2). The regenerated light was sent over the submarine link and compared to the local one to detect the fiber-induced noise after a round trip. FM, Faraday mirrors; PD, photodiodes; AOM, acousto-optic modulators (frequency shifters); EDFA, erbium-doped fiber amplifier (used on L2 only).

deliver the ultra-stable light from the University of Malta to the closest input to the submarine link (landing station). The length of noise-compensated sections was 18 km for L1 and 8 km for L2. This ensures that the high phase stability of the cavity-stabilized laser is preserved for the measurement of the submarine link noise, which took place in the landing station. At the landing station, we regenerated the ultra-stable light using a second fiber laser (laser 2) phase-locked to the incoming light. Two 25 m patch cords connected the regeneration station with the submarine fibers. After a round trip, the light was combined to that injected in the fiber on a photodiode (PD). We performed the phase noise measurements in the landing station rather than at the University of Malta to exclude the noise contribution of the fiber spans on land, which are located in densely populated metropolitan areas. For both testbeds, the loss of each fiber of the pair was 22 dB, leading to a total loss of 44 dB over the round trip. L2 included a bidirectional erbium-doped fiber amplifier (EDFA) with ∼15 dB gain, placed at the far end in Sicily. We used two acousto-optic frequency modulators (AOMs) to perform heterodyne detection between the local and round-trip light. The generated beat note was tracked by a clean-up oscillator, and its phase was sampled with a dead-time-free frequency counter. A low-noise, oven-controlled quartz oscillator served

as a frequency reference for the AOMs feeding frequencies, for the loop-filters and phase-locked loops local oscillators, and for the phase noise measurement. We mounted all equipment in rack-compatible enclosures to support operation in a non-laboratory environment. We housed all fiber components (couplers and Faraday mirrors) in a wooden box filled with foam to reduce their sensitivity to temperature and acoustic noise at the landing station.

The measured round-trip signal exhibited high polarization stability. No polarization adjustments were required over days of operation. In contrast, land-based links of similar length typically require polarization adjustments several times a day. L1 and L2 were installed in 2009 and 2014, respectively. Mechanical stresses in both the silica and polymer coating are likely to have extinguished after several years in the relatively stable underwater environment. We believe this also contributes to the observed polarization stability.

Figure 3(a) shows a comparison of the phase noise power spectral density (PSD) measured on L1 (red line) with previous measurements we performed on other testbeds established on land. The green line shows the phase noise measured over a 2×150 km fiber placed between Turin and Modane, in the French Alps [27], and the black line shows the phase noise of a 2×92 km fiber, which is part of the Italian Link for Frequency and Time and is deployed in North Italy, between Turin and nearby towns [28]. A considerably lower phase noise is observed at all Fourier frequencies. We measured the residual noise of the measurement setup by replacing the submarine cable with fixed attenuator of equivalent loss and leaving the 2×25 m patch cords in place. The measured phase noise in this case is shown by the gray line in Fig. 3(a) and overlaps with that including the submarine cable, establishing an upper bound of the noise introduced by the submarine link. We point out that the patch cords in the server room were suspended above air-conditioned racks hosting equipment with embedded cooling fans and thus exposed to air turbulence and acoustic noise. We expect the noise per unit length of buried fiber to be considerably lower than that of these patch cords. A lower noise floor was observed while performing the measurements on L2 because a much quieter environment was available in this case. More details will be given in Section 3. The peak at around 0.15 Hz observed on the submarine fiber noise is attributed to microseismic noise generated by wind–sea interaction. This aspect will be discussed in Section 5.

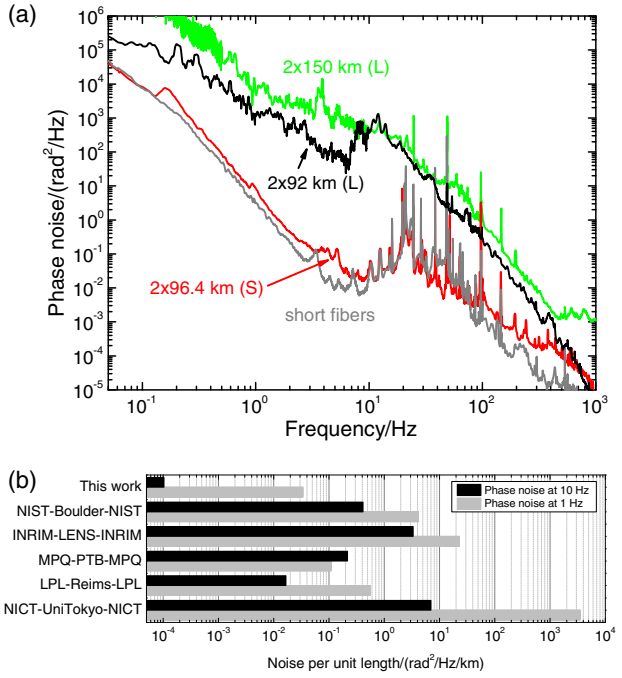

Fig. 3. (a) Round-trip phase noise of various fiber testbeds. Red line: submarine 2×96.4 km link; green line: 2×150 km fiber along highway; black line: 2×92 km fiber along highway (other area). The gray line indicates the noise floor, measured by excluding the submarine cable while leaving the 2×25 m patch cords in place. *L* and *S* indicate land and submarine links, respectively. (b) A comparison of the phase noise per-unit-length of some long-haul links at 1 Hz and 10 Hz. NIST-Boulder-NIST: US, 76 km [20]; INRIM-LENS-INRIM: Italy, 1284 km [9]; MPQ-PTB-MPQ: Germany, 1840 km [31]; LPL-Reims-LPL: France, 540 km [30]; NICT-UniTokyo-NICT: Japan, partly aerial fibers, 114 km [32].

Figure 3(b) shows the noise per-unit-length at 1 Hz and at 10 Hz Fourier frequency for the submarine fiber and some long-haul links established on land. The submarine fiber shows lower noise levels than links on land, the reduction being more than 2 orders of magnitude in the acoustic region at 10 Hz. We expected lower noise from the submarine links. In the acoustic frequency range, the noise of fiber links installed on land is dominated by man-made activities such as road traffic [29]. Large differences are observed among on-land fiber links: the NIST-Boulder-NIST link runs around the town of Boulder (US) [20]; the INRIM-LENS-INRIM link in Italy runs along one of the major highways [9]; the LPL-Reims-LPL link runs between Paris and the town of Reims (France) [30]; the MPQ-PTB-MPQ link in Germany [31] runs next to a gas pipeline. The much higher noise observed on the NICT-UniTokyo-NICT link in Japan is attributed to aerial fibers being used for half of its length [32]. Although measurements on aerial fibers are reported in the literature, no spectral analysis is available [33–35]. Still, all aerial links show worse noise with respect to ground links. This is attributed to a higher exposure to environmental factors such as wind, as fibers are dangling between poles.

Figure 4 shows the frequency stability (overlapping Allan deviation) of L1 over a 24-h-long measurement (black, squares)

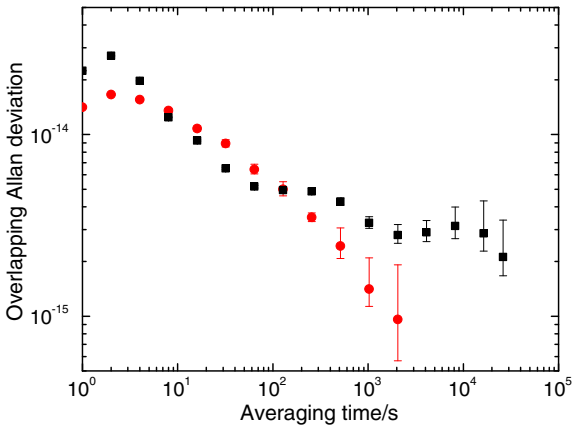

Fig. 4. Frequency instability of the submarine fiber over 24 h (black, squares). Also shown is the instability of the short link composed of the 2×25 m patch cords connecting our apparatus to the submarine cables (red circles).

and the contribution of the short 2 × 25 m patch cords link (red, circles). The data from which it is calculated are sampled at a 1 kHz rate and subsequently averaged by a factor of 1000, and therefore the equivalent measurement bandwidth is 0.5 Hz [36]. The instability excess at short averaging times is attributed to the microseismic peak at 0.15 Hz. Its magnitude changes over time, depending on the environmental conditions. The shown instability corresponds to a case where it was particularly evident. The contribution of the short 2 × 25 m patch cords limits the observed instability up to about 100 s, while for longer measurement times it becomes negligible. In fact, as the server-room temperature is expected to be stable in the long term, the long-term frequency instability is dominated by the round trip in the 192.8 km submarine fiber. After few hours of measurement, it achieves the level of 2×10^{-15}. This extremely low instability is already adequate for many metrological applications based on uncompensated fibers and could be further reduced by enabling noise compensation. This aspect is discussed further in Section 4.

3. PHASE NOISE IN A HIGH-VOLTAGE SUBMARINE CABLE

Similar to land-based links, submarine optical fibers are sometimes placed along oil and gas pipelines or electrical cables up to distances of ∼1000 km. In L2, our fiber was placed inside the interstitial spaces of an HV cable, designed for 245 kV–50 Hz and rated for 655 A. We measured the effect of the electromagnetic fields generated by the strong alternating current on the coherent optical transfer.

A sketch and a picture of the submarine cable cross section are shown in Fig. 5. The three copper cores of the cable are insulated by cross-linked polyethylene (XLPE). A lead alloy sheaths each core and a single-layer steel-wire armor protects the overall structure [25]. Two fiber cables are placed in off-center positions.

In principle, both the phase and the polarization state of the optical field can be affected by the electromagnetic field through the Kerr effect, the Faraday effect, and electrostriction [37,38]. Interaction between electromagnetic and optical signals has been already observed in transmission over suspended fibers [34,35]. However, we show that none of these effects played a role in our experiment (see Supplement 1). Nevertheless, we measured a strong modulation of the optical phase at 100 Hz. We excluded that the modulation was an experimental artifact, as this was not observed either on L1 and when a short link was used instead of the submarine link.

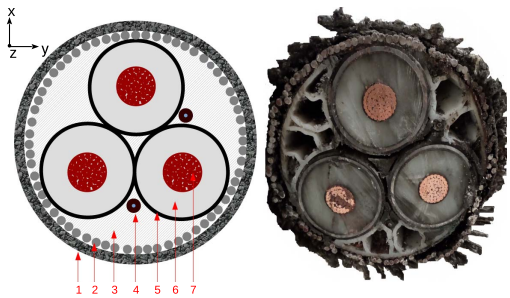

Fig. 5. Simplified sketch (left) and a picture (right) of the cable used in our experiment. 1: external protection, 2: steel-wire armor, 3: filler, 4: optical cables, 5: lead-alloy sheath, 6: cross-linked polyethylene (XLPE) dielectric insulation, 7: copper conductors.

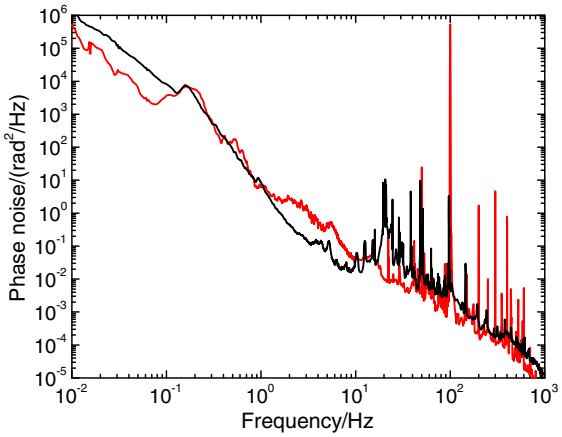

Fig. 6. PSD of the submarine fiber noise on a submarine telecom optical scale (L1, black) and on an optical cable deployed inside a high-voltage submarine power line, also including 19 km of onshore fiber (L2, red).

Figure 6 compares the phase noise of the round-trip signal over the standard telecom cable L1 and the telecom cable embedded in the power line L2. The observed modulation is attributed to the force between current-carrying wires producing a vibration of the cable at twice the line frequency, 100 Hz. Recent studies addressed this issue showing (see, for instance, [39]) that an acoustic tonal noise at twice the line frequency could emerge by more than 20 dB over the background acoustic noise at a distance of 100 m from a submarine HV cable. Assuming a cylindrical spreading law for the sound wave, we estimated the magnitude of the line-synchronous component to be more than 40 dB above the noise close to the source. Although a quantitative estimation is difficult, this effect is consistent with that observed on the optical phase during our experiment on L2, considering that the fiber cable is placed inside the vibrating cable and that the cable itself is buried, thus further shielding the effect of external acoustic noise. The strong modulation of the optical phase could be problematic in some frequency transfer applications as it is only partially suppressed when the noise compensation loop is activated. However, it did not constitute an issue for our phase noise measurements, as its frequency is well within the tracking bandwidth of clean-up filters.

Changes in the electric current flowing in the cables also cause strong variation of the cable temperature. Figure 7(a) shows the expected temperature variations ΔT (black line) of L2, calculated from the observed phase variations $\Delta\phi$ over the round trip through the relation

$$\Delta T = \Delta\phi \Big/ \left(2\pi\nu \frac{2L}{c}\frac{\partial n}{\partial T}\right), \tag{1}$$

where ν and c represent the optical frequency and speed of light in vacuum, L is the link length, and $\frac{\partial n}{\partial T} = 10^{-5}/\mathrm{K}$ is the thermo-optic coefficient [18]. Good agreement is observed with the temperature variations measured by a commercially distributed Brillouin sensor placed along the power cable (red line). This sensor produces space-resolved temperature measurements over the whole cable length, with a 2 m resolution. The trace shown in Fig. 7(a) has been obtained by integrating these point measurements for comparison with the integrated optical phase. The resulting temperature changes are considerably larger than those that would be induced by a typical submarine environment.

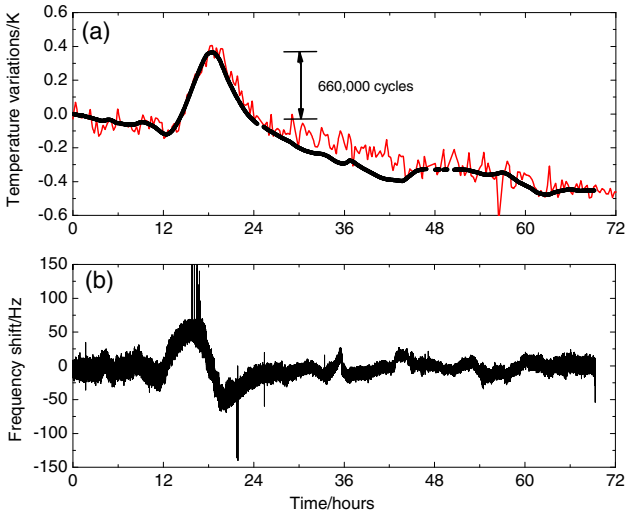

Fig. 7. (a) The temperature variations estimated from the observed phase evolution (black line) and the measured variations obtained by a distributed Brillouin sensor placed along the cable (red line). (b) The corresponding frequency shift.

For example, if we attribute the optical phase variations of L1 exclusively to temperature, the corresponding temperature variations are calculated to be lower than 14 mK. For comparison, in the 2 × 150 km land link shown in Fig. 3, the calculated variations are approximately 1.4 K and exhibit daily periodicity [27]. The temperature changes induced by the high current flowing in the cable were observed to lead to phase variations of up to 6×10^5 cycles in few hours. These correspond to frequency variations as large as 60 Hz or 3×10^{-13}, as shown in Fig. 7(b), which in turns lead to a deterioration of frequency stability. These large phase excursions do not represent a problem in fully bidirectional links, where they are rejected. A different situation might occur in links established with fiber pairs, where one fiber is used for each direction of propagation and the phase changes might not be fully correlated. This could compromise the stability and accuracy of the transferred signal. We note that such temperature effects are likely to be observed also in gas and oil pipelines, whose temperature is often actively changed to regulate the flux of gas or oil. Moreover, these utility distribution systems in most cases control the fluid temperature by electric heating or through induction. This might lead to non-negligible electric and magnetic-field-related effects as observed in our experiment. These sources must be carefully assessed during the design of frequency transfer systems over submarine links.

4. TRANSCONTINENTAL FIBER LINKS FOR METROLOGY

From the noise measurements on the L1 and L2 links, we extrapolate the noise levels that could be found on an intercontinental fiber link of length up to 7000 km. This enables us to calculate the transfer stability that can be achieved in a two-way phase comparison over these distances, when the signals propagate bidirectionally in the same fiber or in two separate fibers, one for each direction of propagation. In order to estimate the noise over intercontinental distances, we make the assumption that the perturbations have a correlation length much shorter than the link length L [20]. We believe this is justified by taking into consideration the local nature of noise-inducing sources like wind, rain, and currents [40]. We also believe our estimate is conservative as it is based on noise levels measured in the shallow and dense traffic-carrying waters of the Sicily–Malta channel, where man-made noise arising from ferries, boats, and coastal activity can have a substantial impact on the seafloor. Over timescales of hours, we expect the noise to be dominated by temperature changes. A proper estimation of their magnitude and correlation length is challenging because of the lack of sufficient literature on hourly or daily temperature variations of the seafloor. However, studies on the seasonal and annual trends show that seafloor temperature fluctuations decrease significantly with depth [41] and are at the level of few tens of milliKelvin in abyssal oceanic plains over a monthly scale [42], and thus we expect them to be significantly lower on the hourly scale that is considered in this work. Under the assumption of spatially uncorrelated perturbations, the power spectral density (PSD) of the measured noise increases linearly with L. This can be written as

$$S_L(f) = \frac{L}{L_0} S_{L_0}(f), \tag{2}$$

where $S_{L_0}(f)$ indicates the phase noise of a link of length L_0.

It should be considered that in our experiment we measured the optical phase noise after a round trip in a 100 km link in two adjacent fibers. It can be demonstrated that the noise of a single trip can be obtained by dividing the round-trip noise by a factor of 4 [20]. This takes into account the fact that the noise in the two directions is highly correlated at Fourier frequencies $f \ll v/L$, where v is the speed of light in the fiber. The residual noise expected when the link is operated in the two-way technique can be predicted if the noise PSD of the fiber $S_\varphi(f)$ is known. The residual noise was calculated for a link where a single fiber is used for both directions of propagation [21]. When separate fibers are used the noise is not fully correlated. To mathematically describe this situation, we assume that two fibers of the same cable are affected by a correlated component, which is common in amplitude and phase for the two fibers, plus an uncorrelated component, whose PSD $S_\delta(f)$ is related to the overall fiber noise $S_\varphi(f)$ through the relation

$$S_\delta(f) = (1 - k)^2 S_\varphi(f), \tag{3}$$

with $0 < k < 1$. This means that the root-mean-square amplitude of the correlated noise is a (usually large) fraction k of the total noise. The value of k depends on the specific structure of the cable in which the fibers are housed and is, in general, a decreasing function of Fourier frequency. It can be shown (see Supplement 1) that the noise PSD of a two-way fiber-based clock comparison where a fiber pair is used, $S_{\mathrm{pair,tw}}(f)$, can be written as

$$S_{\mathrm{pair,tw}}(f) = \frac{1}{4}\left[(1 - k)^2 + \frac{1}{3}\left(2\pi f \frac{L}{v}\right)^2\right] S_\varphi(f). \tag{4}$$

This behavior is confirmed by experimental data [22] and it reduces to the well-known prediction in a single-fiber approach when the noise is fully correlated, i.e., for $k = 1$.

As an example, we derive the power spectral density and Allan deviation of a noise-compensated transoceanic link of length $L = 7000$ km. The gray and light gray curves in Fig. 8 are the measured phase noise and Allan deviation over L1 and L2, respectively. The black line shows the noise model that approximates the

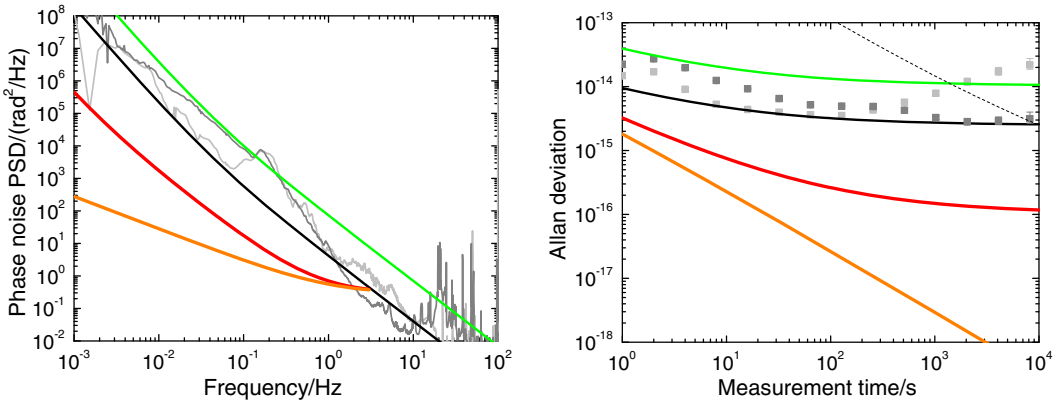

Fig. 8. Phase noise and Allan deviation for various configurations. Gray and light gray: measured values for the L1 and L2 testbeds, established over a ∼100 km looped fiber; black line: mathematical model for the observed noise; green line: extrapolated noise of a free-running 7000 km transoceanic fiber; orange and red lines: expected behavior of a two-way frequency comparison over a 7000 km transoceanic fiber, established over a single fiber or a fiber pair, respectively. The estimated spectra in the graph are plotted only for Fourier frequency $f < 3$ Hz, where the low-frequency approximation is valid.

measured values, described by the power law $S_\varphi(f) = h_{-2}/f^2 + h_{-3}/f^3$ with $h_{-2} = 4$ rad^2 Hz and $h_{-3} = 0.18$ rad^2 Hz^2. The Allan deviation calculated from these values [36] is consistent with that experimentally measured. For the L1 link, the discrepancy at short timescales between the model and the measured values is due to the noise introduced by the 25-m-long patch cords. For the L2 link, the discrepancy occurs at long timescales, where the stability is degraded by the temperature changes induced by the high currents flowing in the HV cable. From this model we evaluated the phase noise and Allan deviation expected for a single-trip 100 km link and then, using Eq. (2), for a transoceanic link. The results are shown by the green line. Finally, we estimate the performance achievable by a two-way comparison scheme in the two approaches where a single or a pair of fibers is used for the two transmitting directions. The red line shows the results in case a fiber pair is used, as derived from Eq. (4). We stress that this relation holds only for Fourier frequencies $f \ll v/L$, which correspond to $f \ll 30$ Hz in a 7000 km link. Accordingly, the estimated spectra in the graph are plotted only for Fourier frequency $f < 3$ Hz. In practical cases, noise at higher frequencies can be effectively rejected by reducing the measurement bandwidth [36]. This estimate uses values of k derived from published measurements on links established over fiber pairs on land. Up to 27 dB rejection has been reported on the noise of the two-way comparison with respect to the noise of the free-running fiber at frequencies higher than 0.1 Hz, implying $k = 0.91$ [22]. A similar value can be derived with an analogous procedure from the measurements reported in [27], which refer to a different topology. The correlation further increases for long-term noise. In [22], the Allan deviation on averaging times of hours is improved by 2 orders of magnitude over that of the uncompensated fiber, meaning that the low-frequency noise rejection can be as high as 40 dB, which corresponds to $k = 0.98$. In our estimate, we assumed $k = 0.91$ at Fourier frequencies $f > 4$ mHz and $k = 0.98$ for lower frequencies. The ultimate instability expected for this link is at the level of 1×10^{-16} and can be reached within few hours of measurement. These results, based on experimental values for the submarine fibers' noise, confirm previous estimations of transoceanic comparisons based on the noise of terrestrial links [22]. The orange lines show the expected performance for the single-fiber approach. As in the previous case, the extrapolated noise is considered only for Fourier frequencies $f < 3$ Hz. Ultimate uncertainties in the 10^{-19} range could be, in principle, achievable, although the feasibility of this kind of architecture still remains to be explored. We show that fiber-based techniques are a viable alternative to satellite-based techniques over transoceanic distances for remote clock comparison. While it is not possible to use traditional bidirectional frequency transfer techniques, the expected correlation of two adjacent fibers enables a transfer stability at the 1×10^{-16} level to be achieved in less than one hour of measurement. In contrast, the best satellite-based techniques (GPS Integer Precise Point Positioning, GPS IPPP) require a few days of measurement [43] to achieve the same level of stability {dashed line [modified Allan deviation] in Fig. 8(b)}. While this is still not sufficient to compare optical clocks at their ultimate performance, much faster comparisons of primary standards over fiber could be achieved using fiber links instead of satellite links, enabling a faster and more accurate computation of the International Atomic Time. Moreover, the combined use of fiber and satellite techniques could help tackle the ultimate limits of both techniques.

We also stress that our noise estimation might be conservative, as environmental noise in the ocean could result to be lower than that measured in the Mediterranean Sea. Both L1 and L2 links are installed in shallow sea and exposed to intense ship traffic and large temperature variations. Lower acoustic noise from shipping and temperature variations can be expected on the ocean floor.

A transoceanic link of up to 7000 km length uses tens of cascaded optical amplifiers to counteract the optical losses. It has been demonstrated that in long amplifiers, chains of their amplified spontaneous emission can build up and degrade the optical signal-to-noise ratio [44]. An impact of this effect on coherent frequency transfer should be considered as well.

5. APPLICATIONS IN GEOPHYSICAL SENSING

The extremely low intrinsic noise of submarine fiber cables in the acoustic region and on timescales of minutes opens a broad range of perspectives for their applications outside the core metrological field, especially for sensing. Almost everywhere, the seafloor is affected by seismic noise at frequencies ranging from 0.1 to 0.2 Hz. This is generally attributed to wind–sea interaction [45], which creates trains of counter-propagating waves. In turns,

the motion of the water column is transmitted to the underlying ground causing a vertical motion, with a micrometer amplitude (hence the name *microseismicity*) at twice the wave frequency. The study of seafloor seismicity through ocean-bottom seismometers (OBS) has proved to be a useful tool for investigating phenomena such as wave formation and propagation [46]. This is of interest for the environmental monitoring of areas where sensing buoys are not available, e.g., open seas and oceans, or as a complementary tool to satellite techniques, which have a coarse spatial coverage and a poor spectral response.

During our measurement campaign, we were able to detect these periodic oscillations at a Fourier frequency of 0.15 Hz. Figure 9 compares the spectrum of the phase acquired by the optical signal while traversing the fiber with that of two seismometers (displacement measurements), located within few kilometers from the link end in Sicily (IV.HPAC) and Malta (MN.WDD). The spectra were recorded at the same time and have been re-normalized for better visualization.

A peak at approximately 0.15 Hz is visible on all traces, whose power was observed to change over the course of a few hours. No correlation was found between the time evolution of this signal among the three measured spectra. We attribute this to the local nature of the perturbation induced by wind and waves, which can substantially vary over the considered distances [46]. In fact, while seismometers measure the seismic displacement at a single location, the signal retrieved from the fiber represents the displacement integrated over the full fiber path.

The use of an optical fiber as a sensing element could be investigated also for the detection of other weak effects such as the Earth's background seismic oscillations in the millihertz spectral region, detected also in the absence of earthquake events, known as *hum* [47]. Researchers are still looking for a satisfactory explanation of this effect, which is complicated by the high background noise of OBS due to ocean wave loads and seafloor currents. On the one hand, post-processing techniques are being proposed to deconvolve these artefacts from the true measurand [48]. A deployed optical fiber, on the other hand, is expected to be less affected than an OBS, thus offering intriguing possibilities also for the study of this effect.

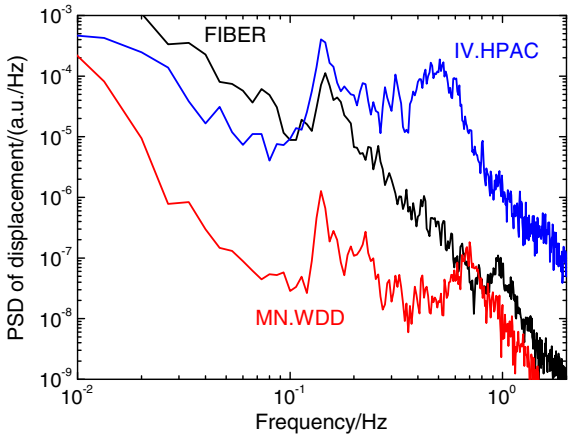

Fig. 9. Black line, "FIBER": the PSD of the optical phase; blue line, "IV.HPAC" the displacement of a seismometer located on the shore in Pachino, Sicily (IV.HPAC); red line, "MN.WDD" the displacement of a seismometer located in Malta (MN.WDD). The spectra were calculated in the same time window and have been re-normalized for better visualization.

6. CONCLUSION

We reported on the first noise characterization of submarine fiber links for frequency metrology. We observed interaction between high-voltage electric fields and measured optical phase in a fiber link installed in a power cable, and we identified the mechanism behind the observed perturbations. These measurements are an essential prerequisite for studying the feasibility of intercontinental fiber links for remote clock comparisons. We showed that, while traditional bidirectional frequency transfer techniques are not directly applicable to the existing underwater cable infrastructure, the noise measured on the Malta–Sicily submarine links indicates that a transfer stability of 1×10^{-16} could still be achieved over thousands of kilometers, enabling faster atomic clock comparisons over intercontinental distances. Further research on longer links and in deeper waters will allow for our estimate to be refined.

Funding. We acknowledge funding by the Ministero dell'Istruzione, dell'Università e della Ricerca (MIUR) through the Progetti Premiali 2015 programme (LABMED); Research, Innovation and Development Trust of the University of Malta; Department for Business, Energy and Industrial Strategy (BEIS) as part of the UK National Measurement System Programme; European Metrology Program for Innovation and Research (EMPIR) Project (15SIB05 OFTEN), which has received funding from the EMPIR programme co-financed by the Participating States and European Union's Horizon 2020 Framework Programme (H2020).

Acknowledgment. The facilities of IRIS Data Services, and specifically the IRIS Data Management Center, were used for access to waveforms, related metadata, and/or derived products used in this study. IRIS Data Services are funded through the Seismological Facilities for the Advancement of Geoscience and EarthScope (SAGE) Proposal of the National Science Foundation under Cooperative Agreement EAR-1261681. We are greatly indebted to Simon Montanaro and Roderick Cassar at Melita Limited, and Saviour Baldacchino, Joseph Vassallo, Joseph Cassar, Jason Vella, Jason Pace, and Sammy Ageli at Enemalta plc for providing us with access to the submarine fiber links. We thank Prof. Massimo Inguscio, President of the Consiglio Nazionale delle Ricerche (CNR), for supporting and encouraging the experiment, as well as Robert Sultana from the University of Malta.

See Supplement 1 for supporting content.

REFERENCES

1. M. Schioppo, R. C. Brown, W. F. McGrew, N. Hinkley, R. J. Fasano, K. Beloy, T. H. Yoon, G. Milani, D. Nicolodi, J. A. Sherman, N. B. Phillips, C. W. Oates, and A. D. Ludlow, "Ultrastable optical clock with two cold-atom ensembles," Nat. Photonics **11**, 48–52 (2017).
2. N. Huntemann, C. Sanner, B. Lipphardt, C. Tamm, and E. Peik, "Single-ion atomic clock with 3×10^{-18} systematic uncertainty," Phys. Rev. Lett. **116**, 063001 (2016).
3. P. Gill, "Is the time right for a redefinition of the second by optical atomic clocks?" J. Phys. **723**, 012053 (2016).
4. T. Takano, M. Takamoto, I. Ushijima, N. Ohmae, T. Akatsuka, A. Yamaguchi, Y. Kuroishi, H. Munekane, B. Miyahara, and H. Katori, "Geopotential measurements with synchronously linked optical lattice clocks," Nat. Photonics **10**, 662–666 (2016).
5. J. Grotti, S. Koller, S. Vogt, S. Hafner, U. Sterr, C. Lisdat, H. Denker, C. Voigt, L. Timmen, A. Rolland, F. N. Baynes, H. S. Margolis, M. Zampaolo, P. Thoumany, M. Pizzocaro, B. Rauf, F. Bregolin, A. Tampellini,

P. Barbieri, M. Zucco, G. A. Costanzo, C. Clivati, F. Levi, and D. Calonico, "Geodesy and metrology with a transportable optical clock," Nat. Phys. **14**, 437–441 (2018).
6. P. Delva, J. Lodewyck, S. Bilicki, E. Bookjans, G. Vallet, R. Le Targat, P.-E. Pottie, C. Guerlin, F. Meynadier, C. Le Poncin-Lafitte, O. Lopez, A. Amy-Klein, W.-K. Lee, N. Quintin, C. Lisdat, A. Al-Masoudi, S. Dörscher, C. Grebing, G. Grosche, A. Kuhl, S. Raupach, U. Sterr, I. R. Hill, R. Hobson, W. Bowden, J. Kronjäger, G. Marra, A. Rolland, F. N. Baynes, H. S. Margolis, and P. Gill, "Test of special relativity using a fiber network of optical clocks," Phys. Rev. Lett. **118**, 221102 (2017).
7. C. Lisdat, G. Grosche, N. Quintin, C. Shi, S. M. F. Raupach, C. Grebing, D. Nicolodi, F. Stefani, A. Al-Masoudi, S. Dörscher, S. Häfner, J.-L. Robyr, N. Chiodo, S. Bilicki, E. Bookjans, A. Koczwara, S. Koke, A. Kuhl, F. Wiotte, F. Meynadier, E. Camisard, M. Abgrall, M. Lours, T. Legero, H. Schnatz, U. Sterr, H. Denker, C. Chardonnet, Y. Le Coq, G. Santarelli, A. Amy-Klein, R. Le Targat, J. Lodewyck, O. Lopez, and P.-E. Pottie, "A clock network for geodesy and fundamental science," Nat. Commun. **7**, 12443 (2016).
8. J. Guéna, S. Weyers, M. Abgrall, C. Grebing, V. Gerginov, P. Rosenbusch, S. Bize, B. Lipphardt, H. Denker, N. Quintin, S. M. F. Raupach, D. Nicolodi, F. Stefani, N. Chiodo, S. Koke, A. Kuhl, F. Wiotte, F. Meynadier, E. Camisard, C. Chardonnet, Y. Le Coq, M. Lours, G. Santarelli, A. Amy-Klein, R. Le Targat, O. Lopez, P. E. Pottie, and G. Grosche, "First international comparison of fountain primary frequency standards via a long distance optical fiber link," Metrologia **54**, 348–354 (2017).
9. D. Calonico, E. K. Bertacco, C. E. Calosso, C. Clivati, G. A. Costanzo, M. Frittelli, A. A. Godone Mura, N. Poli, D. V. Sutyrin, G. M. Tino, M. E. Zucco, and F. Levi, "High-accuracy coherent optical frequency transfer over a doubled 642-km fiber link," Appl. Phys. B **117**, 979–986 (2014).
10. EMPIR project OFTEN—Optical Frequency Transfer—a European Network, https://www.ptb.de/emrp/often_home.html.
11. C. Clivati, R. Ambrosini, T. Artz, A. Bertarini, C. Bortolotti, M. Frittelli, F. Levi, A. Mura, G. Maccaferri, M. Nanni, M. Negusini, F. Perini, M. Roma, M. Stagni, M. Zucco, and D. Calonico, "A VLBI experiment using a remote atomic clock via a coherent fiber link," Sci. Rep. **7**, 40992 (2017).
12. P. Krehlik, Ł. Buczek, J. Kołodziej, M. Lipiński, Ł. Śliwczyński, J. Nawrocki, P. Nogaś, A. Marecki, E. Pazderski, P. Ablewski, M. Bober, R. Ciuryło, A. Cygan, D. Lisak, P. Masłowski, P. Morzyński, M. Zawada, R. M. Campbell, J. Pieczerak, A. Binczewski, and K. Turza, "Fibre-optic delivery of time and frequency to VLBI station," Astron. Astrophys. **603**, A48 (2017).
13. Y. He, K. G. H. Baldwin, B. J. Orr, R. B. Warrington, M. J. Wouters, A. N. Luiten, P. Mirtschin, T. Tzioumis, C. Phillips, J. Stevens, B. Lennon, S. Munting, G. Aben, T. Newlands, and T. Rayner, "Long-distance telecom-fiber transfer of a radio-frequency reference for radio astronomy," Optica **5**, 138–146 (2018).
14. B. Argence, B. Chanteau, O. Lopez, D. Nicolodi, M. Abgrall, C. Chardonnet, C. Daussy, B. Darquié, Y. Le Coq, and A. Amy-Klein, "Quantum cascade laser frequency stabilization at the sub-Hz level," Nat. Photonics **9**, 456–460 (2015).
15. L. F. Livi, G. Cappellini, M. Diem, L. Franchi, C. Clivati, M. Frittelli, F. Levi, D. Calonico, J. Catani, M. Inguscio, and L. Fallani, "Synthetic dimensions and spin-orbit coupling with an optical clock transition," Phys. Rev. Lett. **117**, 220401 (2016).
16. J. Friebe, M. Riedmann, T. Wübbena, A. Pape, H. Kelkar, W. Ertmer, O. Terra, U. Sterr, S. Weyers, and G. Grosche, "Remote frequency measurement of the $^1S_0 1 \rightarrow {}^3P_1$ transition in laser-cooled ^{24}Mg," New J. Phys. **13**, 125010 (2011).
17. A. Matveev, C. G. Parthey, K. Predehl, J. Alnis, A. Beyer, R. Holzwarth, T. Udem, T. Wilken, N. Kolachevsky, M. Abgrall, D. Rovera, C. Salomon, P. Laurent, G. Grosche, O. Terra, T. Legero, H. Schnatz, S. Weyers, B. Altschul, and T. W. Hänsch, "Precision measurement of the hydrogen 1S-2S frequency via a 920-km fiber link," Phys. Rev. Lett. **110**, 230801 (2013).
18. L. G. Cohen and J. W. Fleming, "Effect of temperature on transmission in lightguides," Bell Syst. Tech. J. **58**, 945–951 (1979).
19. C. N. Pannell, J. D. C. Jones, and D. A. Jackson, "The effect of environmental acoustic noise on optical fibre based velocity and vibration sensor systems," Meas. Sci. Technol. **5**, 412–417 (1994).
20. P. A. M. Williams, W. C. Swann, and N. R. Newbury, "High-stability transfer of an optical frequency over long fiber-optic links," J. Opt. Soc. Am. B **25**, 1284–1293 (2008).
21. C. E. Calosso, E. Bertacco, D. Calonico, C. Clivati, G. A. Costanzo, M. Frittelli, F. Levi, A. Mura, and A. Godone, "Frequency transfer via a two-way optical phase comparison on a multiplexed fiber network," Opt. Lett. **39**, 1177–1180 (2014).
22. A. Bercy, F. Stefani, O. Lopez, C. Chardonnet, P.-E. Pottie, and A. Amy-Klein, "Two-way optical frequency comparisons at 5×10^{-21} relative stability over 100-km telecommunication network fibers," Phys. Rev. A **90**, 061802(R) (2014).
23. S.-C. Ebenhag, K. Jaldehag, C. Rieck, P. Jarlemark, P. O. Hedekvist, P. Löthberg, T. Fordell, and M. Merimaa, "Time transfer between UTC(SP) and UTC(MIKE) using frame detection in fiber-optical communication networks, " in *Proceedings of the 43rd Annual Precise Time and Time Interval Systems and Applications Meeting*, Long Beach, California (2011), pp. 431–442.
24. M. Amemiya, M. Imae, Y. Fujii, T. Suzuyama, and S. Ohshima, "Simple time and frequency dissemination method using optical fiber network," IEEE Trans. Instrum. Meas. **57**, 878–883 (2008).
25. S. Lauria and F. Palone, "Operating envelopes of the Malta-Sicily 245 KV-50 HZ cable," in *2nd IEEE ENERGYCON Conference & Exhibition, 2012/Future Energy Grids and Systems Symp.* (2012), pp. 287–292.
26. K. Numata, A. Kemery, and J. Camp, "Thermal-noise limit in the frequency stabilization of lasers with rigid cavities," Phys. Rev. Lett. **93**, 250602 (2004).
27. A. Tampellini, C. Clivati, D. Calonico, A. Mura, and F. Levi, "Effect of a timebase mismatch in two-way optical frequency transfer," Metrologia **54**, 805–809 (2017).
28. C. Clivati, G. Bolognini, D. Calonico, S. Faralli, A. Mura, and F. Levi, "In-field Raman amplification on coherent optical fiber links for frequency metrology," Opt. Express **23**, 10604–10615 (2015).
29. L. Sliwczynski and P. Krehlik, "Measurement of acoustic noise in field-deployed fiber optic cables," in *European Frequency and Time Forum (EFTF)*, Neuchatel, Switzerland (2014), pp. 339–342.
30. O. Lopez, A. Haboucha, B. Chanteau, C. Chardonnet, A. Amy-Klein, and G. Santarelli, "Ultra-stable long distance optical frequency distribution using the Internet fiber network," Opt. Express **20**, 23518–23526 (2012).
31. S. Droste, F. Ozimek, T. Udem, K. Predehl, T. W. Hansch, H. Schnatz, G. Grosche, and R. Holzwarth, "Optical-frequency transfer over a single-span 1840 km fiber link," Phys. Rev. Lett. **111**, 110801 (2013).
32. M. Fujieda, M. Kumagai, and S. Nagano, "Coherent microwave transfer over a 204-km telecom fiber link by a cascaded system," IEEE Trans. Ultrason. Ferroelectr. Freq. Control **57**, 168–174 (2010).
33. D. Gozzard, S. W. Schediwy, B. Wallace, R. Gamatham, and K. Grainge, "Characterization of optical frequency transfer over 154 km of aerial fiber," Opt. Lett. **42**, 2197–2200 (2017).
34. S.-C. Ebenhag, P. O. Hedekvist, and L. Weddig, "Measurement and analysis of polarization variations in an optical coherent fiber communication network utilized for time and frequency distribution," in *Proceedings of the 49th Annual Precise Time and Time Interval Systems and Applications Meeting*, Reston, Virginia (2018), pp. 233–236.
35. L. Sliwczynski, P. Krehlik, K. Turza, and A. Binczewski, "Characterization of the frequency transfer over 300 km of aerial suspended fiber, " in *European Frequency and Time Forum (EFTF)*, York, UK (2016).
36. C. Calosso, C. Clivati, and S. Micalizio, "Avoiding aliasing in Allan variance: an application to fiber link data analysis," IEEE Trans. Ultrason. Ferroelectr. Freq. Control **63**, 646–655 (2016).
37. A. Melloni, M. Frasca, A. Garavaglia, A. Tonini, and M. Martinelli, "Direct measurement of electrostriction in optical fibers," Opt. Lett. **23**, 691–693 (1998).
38. J. Prat and J. Comellas, "Dispersion-shifted fiber polarization scrambler based on Faraday effect," IEEE Photon. Technol. Lett. **11**, 845–847 (1999).
39. Vancouver Island Transmission Reinforcement Project: Atmospheric and Underwater Acoustics Assessment, Report prepared for British Columbia Transmission Corporation (2006), p. 49.
40. C. Erbe, A. Verma, R. McCauley, A. Gavrilov, and I. Parnum, "The marine soundscape of the Perth Canyon," Progr. Oceanogr. **137**, 38–51 (2015).
41. W. H. K. Lee and C. S. Cox, "Time variation of ocean temperatures and its relation to internal waves and oceanic heat flow measurements," J. Geophys. Res. **71**, 2101–2111 (1966).
42. H. W. Broek, "Bottom temperature fluctuations on the continental slope of the Northwest Atlantic Ocean," J. Phys. Oceanogr. **35**, 388–394 (2005).
43. G. Petit, A. Kanj, S. Loyer, J. Delporte, F. Mercier, and F. Perosanz, "1×10^{-16} frequency transfer by GPS PPP with integer ambiguity resolution," Metrologia **52**, 301–309 (2015).

44. C. Delisle and J. Conradi, "Model for bidirectional transmission in an open cascade of optical amplifiers," J. Lightwave Technol. **15**, 749–757 (1997).
45. K. Hasselmann, "A statistical analysis of the generation of micro-seisms," Rev. Geophys. **1**, 177–210 (1963).
46. F. Ardhuin, A. Balanche, E. Stutzmann, and M. Obrebski, "From seismic noise to ocean wave parameters: general methods and validation," J. Geophys. Res. **117**, C05002 (2012).
47. K. Nishida, N. Kobayashi, and Y. Fukao, "Resonant oscillations between the solid Earth and atmosphere," Science **287**, 2244–2246 (2000).
48. M. Deen, E. Wielandt, E. Stutzmann, W. Crawford, G. Barruoll, and K. Sigloch, "First observation of the Earth's permanent free oscillations on ocean bottom seismometers," Geophys. Res. Lett. **44**, 10988–10996 (2017).